Journal of Engineering Physics and Thermophysics, Vol. 80, No. 3, 2007

THEORETICAL INVESTIGATION OF THE PROCESS OF CLEANING OIL-POLLUTED SOIL IN HYDROCYCLONE APPARATUSES

O. V. Matvienko and E. V. Evtyushkin

UDC 621.928.37

On the basis of the Reynolds equations, a numerical investigation of the flow and separation of oil-polluted soil particles in a hydrocyclone has been conducted. It has been shown that as a result of the hydrocycloning it is possible to concentrate the pollutant in a negligible quantity of soil (of the order of a few percent), which permits reducing its cleaning costs.

Introduction. The problem of hydrocyclone separation of particles of asoil polluted with oil and oil products is considered. Modelling of the separation process is carried out taking into account the following assumptions:

1) as a result of the soil pollution with oil, the latter wraps its particles in a thin film whose thickness l in the case of a low concentration of oil is approximately proportional to the pollutant concentration; thus, the polluted fragment of the soil can be considered as a combination of unadsorbed oil and particles covered with an oil film;

2) a three-phase mixture containing, in addition to the carrier liquid (water), oil droplets and soil particles covered with an oil film is fed into the hydrocyclone from the feeding branch pipe;

3) the three-dimensional effects are manifested only in a relatively small region in the vicinity of the conveying branch pipe, and in the main body of the hydrocyclone the flow is almost axisymmetric [1]; therefore, the changes in the parameters in the tangential direction can be neglected to simplify the mathematical model are reduce the volume of calculations.

Mathematical Model. To describe the hydrodynamics and the transfer processes in the hydrocyclone, the physicomathematical model was used [2–4]. To describe the flow fields, one uses the two-dimensional axisymmetric Reynolds equations that are best suited for describing the axisymmetric flow conditions [5]:

$$\frac{\partial \rho u}{\partial x} + \frac{1}{r}\frac{\partial \rho v r}{\partial r} = 0\,, \tag{1}$$

$$\frac{\partial \rho u^2}{\partial x} + \frac{1}{r}\frac{\partial \rho u v r}{\partial r} = -\frac{\partial p}{\partial x} + \frac{\partial}{\partial x}\left[\mu_{\text{ef}}\left(2\frac{\partial u}{\partial x} - \frac{2}{3}\left(\frac{\partial u}{\partial x} + \frac{1}{r}\frac{\partial v r}{\partial r}\right)\right)\right] + \frac{1}{r}\frac{\partial}{\partial r}\left[\mu_{\text{ef}} r\left(\frac{\partial u}{\partial r} + \frac{\partial v}{\partial x}\right)\right], \tag{2}$$

$$\frac{\partial \rho u v}{\partial x} + \frac{1}{r}\frac{\partial \rho v^2 r}{\partial r} = -\frac{\partial p}{\partial r} + \frac{\partial}{\partial x}\left[\mu_{\text{ef}}\left(\frac{\partial v}{\partial x} + \frac{\partial u}{\partial r}\right)\right] + \frac{1}{r}\frac{\partial}{\partial r}\left[\mu_{\text{ef}} r\left(2\frac{\partial v}{\partial r} - \frac{2}{3}\left(\frac{\partial u}{\partial x} + \frac{1}{r}\frac{\partial v r}{\partial r}\right)\right)\right] - 2\frac{\mu_{\text{ef}} v}{r^2} + \frac{\rho w^2}{r}\,, \tag{3}$$

$$\frac{\partial \rho u w}{\partial x} + \frac{1}{r}\frac{\partial \rho v w r}{\partial r} = \frac{\partial}{\partial x}\left[\mu_{\text{ef}}\frac{\partial w}{\partial x}\right] + \frac{1}{r^2}\frac{\partial}{\partial r}\left[\frac{\mu_{\text{ef}}}{\sigma_{r\varphi}} r^3 \frac{\partial}{\partial r}\left(\frac{w}{r}\right)\right] - \frac{\rho v w}{r}\,. \tag{4}$$

The turbulence characteristics were calculated on the basis of the two-parameter model with the use of balance equations for the kinetic energy of turbulence k and its dissipation rate ε [5]:

Tomsk State Architectural-Building University, 2 Solyanaya Sq., Tomsk, 634003, Russia; email: matvolegv@mail.ru. Translated from Inzhenerno-Fizicheskii Zhurnal, Vol. 80, No. 3, pp. 72–80, May–June, 2007. Original article submitted July 29, 2005; revision submitted June 1, 2006.

$$\frac{\partial \rho u k}{\partial x}+\frac{1}{r}\frac{\partial \rho v k r}{\partial r}=\frac{\partial}{\partial x}\left[\frac{\mu_{ef}}{\sigma_k}\frac{\partial k}{\partial x}\right]+\frac{1}{r}\frac{\partial}{\partial r}\left[\frac{\mu_{ef}}{\sigma_k}r\frac{\partial k}{\partial r}\right]+G-\rho\varepsilon\,, \tag{5}$$

$$\frac{\partial \rho u \varepsilon}{\partial x}+\frac{1}{r}\frac{\partial \rho v \varepsilon r}{\partial r}=\frac{\partial}{\partial x}\left[\frac{\mu_{ef}}{\sigma_\varepsilon}\frac{\partial \varepsilon}{\partial x}\right]+\frac{1}{r}\frac{\partial}{\partial r}\left[\frac{\mu_{ef}}{\sigma_\varepsilon}\frac{\partial \varepsilon}{\partial r}\right]+(C_1G-C_2\rho\varepsilon)\frac{\varepsilon}{k}\,, \tag{6}$$

$$G_k=\mu_t\left\{2\left[\left(\frac{\partial u}{\partial x}\right)^2+\left(\frac{\partial v}{\partial r}\right)^2+\left(\frac{v}{r}\right)^2\right]+\left(\frac{\partial u}{\partial r}+\frac{\partial v}{\partial x}\right)^2+\left(\frac{\partial w}{\partial x}\right)^2+\left(r\frac{\partial w/r}{\partial r}\right)^2\right\}.$$

The values of the constants are chosen in accordance with the recommendations of [6]:

$$C_1=1.44\,,\quad C_2=1.92\,(1-C_3\mathrm{Ri})\,,\quad C_3=0.001\,,\quad \sigma_k=1\,,\quad \sigma_\varepsilon=1.3\,,\quad \sigma_{r\varphi}=2.5\,,\quad \mathrm{Ri}=\frac{k}{\varepsilon^2}\frac{w^2}{r}\frac{\partial\,(wr)}{\partial r}\,.$$

To determine the drift velocity of particles relative to the suspension, balance between the mass forces acting on the particle and the drag forces was assumed [2]. According to the principle of dynamic balance of forces, the velocity of the disperse phase relative to the carrier liquid can be defined as

$$\mathbf{V}_{rel}=\frac{4}{3}d_p^2\frac{\rho_p-\rho_{liq}}{\mu_{liq}C_d\mathrm{Re}_{rel}}\cdot\mathbf{a}_p\,,\quad \mathbf{a}_p=\left\{g,\frac{(w_p)^2}{r},-\frac{v_pw_p}{r}\right\}. \tag{7}$$

The resistance coefficient of a solid sphere of diameter d_p covered with a thin film of length l is defined as [7, 8]

$$C_d=\chi C_{d,p}\,, \tag{8}$$

$$C_{d,p}=\frac{24}{\mathrm{Re}_{rel}}+\frac{3.73}{\sqrt{\mathrm{Re}_{rel}}}-\frac{4.83\cdot10^{-3}\sqrt{\mathrm{Re}_{rel}}}{1+3\cdot10^{-6}\sqrt{\mathrm{Re}_{rel}}}+0.49\,,\quad \chi=\frac{2}{3}\frac{\mu_{liq}+3\mu_{oil}F(\lambda)}{\mu_{liq}+2\mu_{oil}F(\lambda)}\,,$$

$$\mathrm{Re}_{rel}=\rho_{liq}\left|\mathbf{V}_{rel}\right|d_p/\mu_{liq}\,,\quad \lambda=2l/d_p\,,\quad F(\lambda)=\frac{2+\lambda}{\lambda}\frac{1+\lambda+0.4\lambda^2}{3+3\lambda+0.8\lambda^2}\,.$$

Note that with decreasing thickness of the film ($\lambda\to0$) the resistance coefficient of the particle covered with an oil film tends to the values obtained for solid particles: $C_d\to C_{d.p}$. In the other limiting case ($\lambda\to\infty$), formula (8) goes over into the resistance law of liquid droplets defined by the Hadamard–Rybchinskii correction [9]. In this case, the resistance coefficient is written as

$$C_d=\left(1-\frac{1}{3}\frac{\mu_{liq}}{\mu_{oil}+\mu_{liq}}\right)C_{d,p}\,.$$

The mass balance of the solid phase was determined by means of the diffusion equation that describes the convective transfer of particles by the averaged flow and the stochastic motion of particles as a consequence of turbulent pulsations (turbulent diffusion):

$$\frac{\partial\rho\,(u+u_{rel})\,M_j}{\partial x}+\frac{1}{r}\frac{\partial\rho\,(v+v_{rel})\,rM_j}{\partial r}=\frac{\partial}{\partial x}\left[\rho D_p\frac{\partial M_j}{\partial x}\right]+\frac{1}{r}\frac{\partial}{\partial r}\left[\rho D_p\frac{\partial M_j}{\partial r}\right]. \tag{9}$$

The turbulent diffusion coefficient of particles was calculated in a similar manner [10]. In the case of turbulent pulsations causing the particle motion described by the Stokes law of resistance ($\mathrm{Re_t} = \rho\sqrt{k}d_\mathrm{p}/\mu > 1$), the turbulent diffusion coefficient of particles can be defined as

$$D_\mathrm{p} = D_\mathrm{t}\left\{1 - \frac{1}{2\alpha}\frac{d_\mathrm{p}}{L}\left[3 - \exp\left(-\alpha\frac{L}{d_\mathrm{p}}\right)\right]\left[1 - \exp\left(-\alpha\frac{L}{d_\mathrm{p}}\right)\right]\right\}, \tag{10}$$

where $L = k^{3/2}/\varepsilon$, $\alpha = 18\,\frac{\rho}{\rho_\mathrm{p}}\chi\mathrm{Re_t^{-1}}$. In the transition region ($1 < \mathrm{Re_t} \le 10^3$), to determine the turbulent diffusion coefficient of particles, one can use the relation

$$D_\mathrm{p} = D_\mathrm{t}\left\{1 + \frac{\rho_\mathrm{p}}{\rho}\chi^{-1}\frac{d_\mathrm{p}}{L}\sqrt{6}\left[\arctan\sqrt{z_1} - \arctan\sqrt{z_2} + \arctan\sqrt{z_3} - \arctan\sqrt{z_4} + \frac{1}{\sqrt{z_1}} - \frac{1}{\sqrt{z_2}} + \frac{1}{\sqrt{z_3}} - \frac{1}{\sqrt{z_4}}\right]\right\}. \tag{11}$$

The parameters z_1, z_2, z_3, and z_4 in (11) are found in the following way:

$$z_1 = \left(6\mathrm{Re_t^{-2/3}} + 1\right)\exp\left(\frac{12}{\mathrm{Re_t}}\frac{\rho}{\rho_\mathrm{p}}\chi\frac{L}{d_\mathrm{p}}\right) - 1\,; \quad z_2 = 6\mathrm{Re_t^{-2/3}}\,;$$

$$z_3 = 6\left[\frac{1}{6} + \left(2\mathrm{Re_t} - \left(\mathrm{Re_t^{-2/3}} + \frac{1}{6}\right)\exp\left(\frac{12}{\mathrm{Re_t}}\frac{\rho}{\rho_\mathrm{p}}\chi\frac{L}{d_\mathrm{p}}\right) - \frac{1}{6}\right)^{-1.5}\right]^{-2/3}\exp\left(\frac{12}{\mathrm{Re_t}}\frac{\rho}{\rho_\mathrm{p}}\chi\frac{L}{d_\mathrm{p}}\right) - 1\,;$$

$$z_4 = 6\left[\frac{1}{6} + \left(2\mathrm{Re_t} - \left(\mathrm{Re_t^{-2/3}} + \frac{1}{6}\right)\exp\left(\frac{12}{\mathrm{Re_t}}\frac{\rho}{\rho_\mathrm{p}}\chi\frac{L}{d_\mathrm{p}}\right) - \frac{1}{6}\right)^{-1.5}\right]^{-2/3} - 1\,.$$

In the case of the Newtonian flow conditions ($10^3 < \mathrm{Re_t} \le 2\cdot10^5$), the turbulent diffusion coefficient is defined by the relation

$$D_\mathrm{p} = D_\mathrm{t}\left\{1 - \frac{1}{2\beta}\left(\frac{d_\mathrm{p}}{L}\right)\ln\left[1 + 2\beta\left(\frac{L}{d_\mathrm{p}}\right) + 2\left(\beta\frac{L}{d_\mathrm{p}}\right)^2\right]\right\}, \tag{12}$$

where $\beta = \frac{4}{3}\frac{\rho_\mathrm{p}}{\rho}\chi^{-1}\frac{1}{C_\mathrm{d}(\mathrm{Re_{rel}} \to \infty)}$. We assume the resistance coefficient with the relative Reynolds number tending to infinity to be equal to $C_\mathrm{d}(\mathrm{Re_{rel}} \to \infty) = 0.44$.

The suspension density and viscosity depend on the current concentration of the solid phase (and it is assumed thereby that the presence of the solid phase influences the flow structure only in terms of the change in the suspension density and viscosity). The suspension density was determined in terms of the mass fractions and densities of particles of different fractions, as well as of the water:

$$\rho = \left[\frac{1}{\rho_\mathrm{liq}}\left(1 - \sum_{j=1}^{N} M_j\right) + \sum_{j=1}^{N}\frac{M_j}{\rho_{\mathrm{p},j}}\right]^{-1}. \tag{13}$$

The effective viscosity (μ_ef) is determined as a sum of the suspension molecular viscosity (μ_sl) and the turbulent viscosity (μ_t). The quantity μ_sl is considered as a function of the molecular viscosity of the carrier medium (water). (μ_liq) and the total concentration of the solid phase [1]

$$\frac{\mu_{sl}}{\mu_{liq}} = 1 + 2.5\sum_{j=1}^{N} M_j \frac{\rho}{\rho_{p,j}} + 0.0275\sum_{j=1}^{N}\left(M_j \frac{\rho}{\rho_{p,j}}\right)^2 \exp\left(16.6\sum_{j=1}^{N} M_j \frac{\rho}{\rho_{p,j}}\right). \quad (14)$$

Formula (14) was written for the case where the particle densities of different fractions are unequal. The turbulent viscosity can be calculated with the use of the k–ε model of turbulence [5]:

$$\mu_t = C_\mu \rho k^2 \varepsilon^{-1}, \quad C_\mu = 0.09. \quad (15)$$

Because of the ellipticity of the system of differential equations, to close the problem, one has to set the boundary conditions at all boundaries of the calculated region. The inlet boundary conditions (in the feeding branch pipe) are determined for all variables. For the problem to be two-dimensional, it is supposed that the inlet into the hydrocyclone represents a cylindrical surface whose height is chosen to be equal to the diameter of the feeding branch pipe. The inlet kinetic energy of turbulence is taken to be proportional to the kinetic energy of the averaged flow. Thus, the boundary conditions at the inlet are formulated as

$$v_{in} = \frac{Q_{in}}{\pi d_c d_{in}\rho}, \quad u_{in} = \frac{\gamma Q_{in}}{\pi d_c d_{in}\rho}, \quad w_{in} = \frac{4Q_{in}}{\pi d_{in}^2 \rho}, \quad k = \mathrm{Tu}\, w_{in}^2, \quad \varepsilon = \frac{2k_{in}^{3/2}}{\eta d_c}, \quad M_j = M_{j,in}.$$

Here, $\gamma = 0.15$, $\eta = 0.005$, $\mathrm{Tu} = 0.03$ are model constants.

At present, in the technical literature [11–14] there is a large number of empirical formulas for determining the capacities of hydrocyclones Q_{in} or the quantity of suspension that the hydrocyclone can process per unit time. Many of these formulas are of the form

$$Q_{in} = C_Q \rho d_{in} d_{of} \sqrt{\frac{p}{\rho}}$$

and differ from one another by the values of the constant C_Q, which, according to the data of different authors, is in the range of $0.2 \le C_Q \le 0.4$. In the present appear, the value of $C_Q = 0.27$ proposed in [14] is used.

On the symmetry axis, the radial components of gradients of all functions, except for the radial and tangential velocities that are equal to zero here, are assumed to be equal to zero:

$$r = 0: \quad v = 0, \quad \frac{\partial u}{\partial r} = 0, \quad w = 0, \quad \frac{\partial k}{\partial r} = 0, \quad \frac{\partial \varepsilon}{\partial r} = 0, \quad \frac{\partial M_j}{\partial r} = 0.$$

On the hydrocyclone walls, the adhesion and nonpercolation conditions are modeled. To determine the turbulent characteristics, local equilibrium in the wall-adjacent region is assumed:

$$v = 0, \quad u = 0, \quad w = 0, \quad \frac{\partial M_j}{\partial n} = 0, \quad k_{nw} = \frac{\tau_w}{\rho\sqrt{C_\mu}}, \quad \varepsilon_{nw} = \frac{k_{nw}^{3/2} C_\mu^{3/4}}{\kappa r_{nw}},$$

where n is the direction of the normal to the wall. The wall stress τ_w can be determined as

$$\tau_w = \begin{cases} \mu u/(R_c - r_{nw}) & \text{at } Y \le 11.5, \\ EYC_\mu^{0.25}\rho u/\sqrt{k}\,\ln(Y)/\kappa & \text{at } Y > 11.5, \end{cases}$$

where $\kappa = 0.4$; $E = 9.0$ (for a smooth wall); $Y = \sqrt[4]{C_\mu}\,\rho\sqrt{k}(R_c - r_{nw})/\mu$.

At the outlet from the hydrocyclone (in both the overflow and underflow launders), the axial components of the tangential velocity gradients, as well as of the turbulent characteristics k and ε, are assumed to be equal to zero. The values of the radial velocity v in the outlet cross-sections are taken to be equal to zero. The pressure p in the

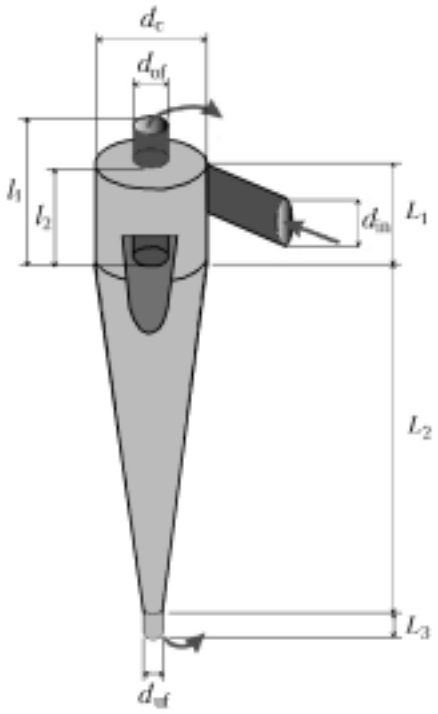

Fig. 1. Scheme of the hydrocyclone.

overflow launder is determined from the assumption of radial equilibrium of the flow, whereas the pressure in the underflow launder is assumed to be equal to atmospheric pressure. Thus, in the outlet cross-sections the boundary conditions can be written as

$$v = 0\,, \quad \frac{\partial p}{\partial r} = \frac{\rho w^2}{r} \quad \text{(overflow launder)}\,, \quad p = 0 \quad \text{(underflow launder)}\,, \quad \frac{\partial w}{\partial x} = 0\,, \quad \frac{\partial k}{\partial x} = 0\,,$$

$$\frac{\partial \varepsilon}{\partial x} = 0\,, \quad \frac{\partial M_j}{\partial x} = 0\,.$$

The procedure of solving the above mathematical model is based on the solution of the system of Reynolds equations in dynamic variables. The finite-difference analog of differential equations was obtained by their integration inside the control volume of the finite-difference mesh. In the calculations, we used displaced meshes with 100 nodes in the radial direction and 300 nodes in the axial one. In approximating the convective terms, counterflow differences with the application of the QUICK scheme were used. In modeling the diffusion terms, the exponential approximation was used. The system of finite-difference equations is nonlinear, and we used the iteration method for solving it. In each iteration, longitudinal-transverse run was used. The pressure was calculated by means of the SIMPLE iteration procedure [15].

Results of the Calculations. On the basis of the mathematical model presented above, a numerical investigation of the flow structure in the hydrocyclone has been conducted (Fig. 1). The design parameters of the apparatus had values corresponding to the experiments of [1–4]: d_c = 75 mm, d_{in} = 25 mm, d_{of} = 25 mm, d_{uf} = 12.5 mm, L_1 = 75 mm, L_2 = 200 mm, L_3 = 25 mm, l_1 = 100 mm, and l_2 = 50 mm.

Consider first the features of the separation of oil droplets in the hydrocyclone. The calculations were performed for droplets distributed in accordance with the Rozin–Ramler distribution function [9]

$$\Psi\,(d_p) = 1 - \exp\left[-\left(\frac{d_p}{\delta}\right)^m\right], \tag{16}$$

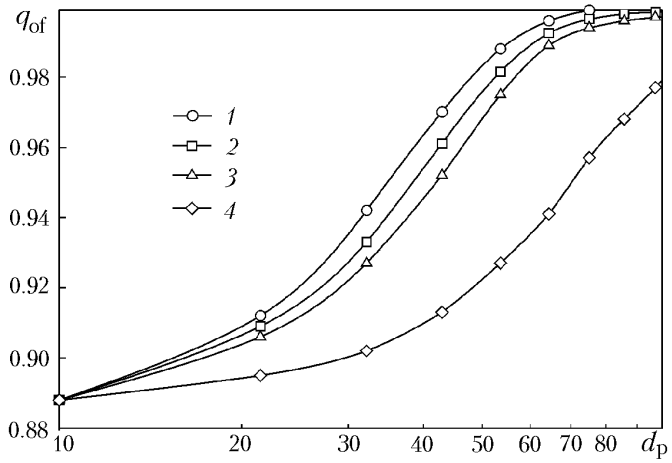

Fig. 2. Separation curves (yield at the overflow) of oil drops of various diameters d_p (p = 1.013·10^5 Pa, d_m = 50 μm): 1) ρ_{oil} = 650; 2) 750; 3) 850; 4) 950 kg/m^3. d_p, μm.

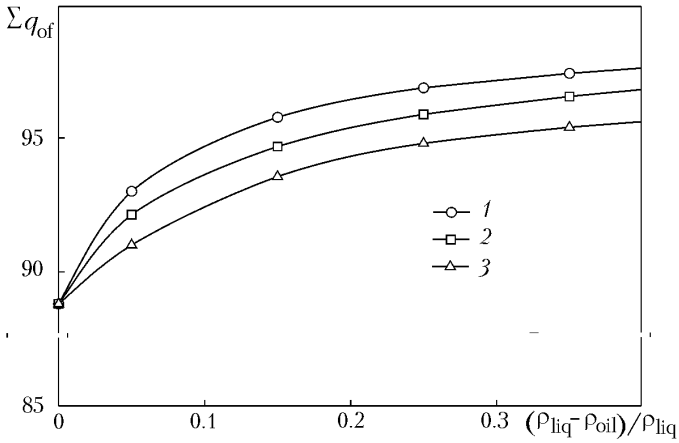

Fig. 3. Total yield of oil droplets through the overflow launder (p = 1.013·10^5 Pa): 1) d_m = 60; 2) 50; 3) 40 μm.

where $\delta = d_m/\sqrt[m]{\ln 2}$. In the calculations, the values of the distribution parameters were assumed to be as follows: d_m = 40–60 μm and m = 2.

The particle velocity of small fractions relative to the carrier liquid is rather small, and the processes of turbulent diffusion are rather intensive. As a result of this, the distribution of the concentrations of small droplets is uniform. Large oil droplets that are lighter than the carrier liquid (water) move from the feeding branch pipe to the hydrocyclone center and then leave it mainly through the overflow launder. As a result, the concentration of oil droplets with their increasing diameter in the overflow launder increases. At the same time, the fraction of oil droplets leaving the hydrocyclone through the underflow launder sharply decreases and for droplets of diameter more than d_p = 50 μm becomes practically equal to zero.

Calculating the flows of each fraction of droplets through the overflow and underflow launders, we can obtain the separation curve (concentration of a certain fraction getting into the launder as a function of the droplet size of this fraction d_p):

$$q_{of}(d_p) = Q_{of}(d_p)/Q_{in}(d_p),$$

where Q_{of} (d_p) and Q_{in} (d_p) are the mass flows of oil droplets in the overflow launder and in the feeding branch pipe. The results of such calculations for various values of the oil density ρ_{oil} are presented in Fig. 2. It is seen that with

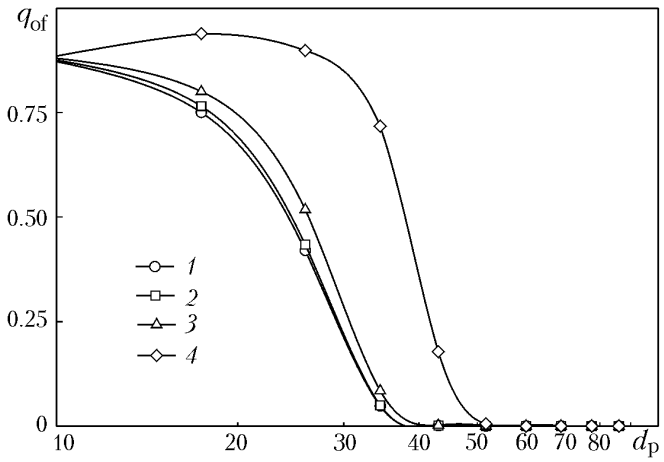

Fig. 4. Separation curves (yield at the overflow) of polluted particles of various diameters d_p (p = 1.013·10^5 Pa): 1) l = 0; 2) 0.1; 3) 1; 4) 10 μm. d_p, μm.

increasing oil density the separation efficiency decreases, which is due to the decrease in the density difference between the droplets and the carrier liquid. The most effective separation is observed for light oil with a density of ρ_{oil} = 650 kg/m^3. For heavy oil with a density of 950 < ρ_{oil} < 1050 kg/m^3, the separation efficiency is determined by the design features of the hydrocyclone and the regime characteristics of the hydrocycloning process.

Summing up the output of each fraction through the overflow launder, one can determine the total yield of oil through the drain hole Σq_{of}. The dependence of the total yield of oil on the relative density difference $(\rho_{liq} - \rho_{oil})/\rho_{liq}$ for various values of the median diameter d_m is shown in Fig. 3. As is seen from this figure, an increase in d_m, meaning an increase in the fraction of large droplets, leads to an increase in the quantity of oil carried off by the overflow launder. This shows up most vividly for light oil.

Summarizing the analysis of the separation of oil droplets in the hydrocyclone, it may be concluded that about 90% of the oil contained in the fed suspension in the form of droplets are carried off by the overflow launder and only 10% by the underflow launder. This points to a high efficiency of the hydrocycloning method.

Consider now the results of the investigation of the particle separation of an oil-polluted soil. As mentioned above, it is considered that the soil particles are covered with an oil film of thickness l. Thus, the diameter of a polluted particle can be defined as $d = d_p + l$. It is assumed that the soil particles are distributed in accordance with the Rozin–Ramler function with the following parameter values: d_m = 40 μm and m = 2. The mean density of an oil-polluted particle is determined as

$$\rho_{ef} = \rho_{oil} + \frac{\rho_p - \rho_{oil}}{(1 + \lambda)^3}. \qquad (17)$$

A decrease in the effective density of oil-polluted particles of small fractions with increasing l promotes their carrying off into the overflow launder and their accumulation in the central part of the discharge pipe. The presence of an oil film on the particles of large fractions practically has no effect on their separation, since the change in the effective density in this case is rather small. The particle yield at the overflow launder for various values of the oil film thickness l is shown in Fig. 4. In the absence of pollution or in the case of an insignificant pollution $\lambda < 0.1$, the separation curve in semilogarithmic coordinates has the Gaussian form.

In the case of significant pollution, the separation curve is characterized by the presence of a maximum corresponding to the particles of medium fractions. The reason for the nonmonotonicity of the separation curve is as follows. The highly polluted small particles can be considered as droplets with a small inclusion of the solid phase. Therefore, their separation is analogous to the separation of droplets: with increasing size of particles their yield into the overflow launder increases. However, this analogy holds only to a certain limit. As soon as the effective density of the particle exceeds the carrier liquid density, the separation process changes: now an increase in the particle size promotes their carrying off by the underflow launder.

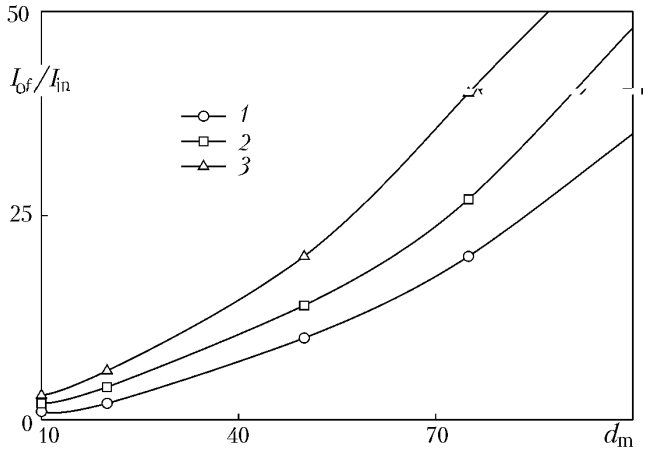

Fig. 5. Relative pollution intensity in the overflow: 1) $p = 1.013 \cdot 10^5$; 2) $2.026 \cdot 10^5$; 3) $3.039 \cdot 10^5$ Pa. d_m, m.

Below we present the results of the investigation that permit estimating the efficiency of using the hydrocycloning method for the problems of cleaning the oil-polluted soil. As a parameter characterizing the degree of soil pollution, we use the ratio of the mass fraction of the oil to the mass fraction of the soil:

$$I = \frac{M_{oil}}{\sum_{j=1}^{N} M_j}.$$

Figure 5 gives the dependence of the relative pollution intensity in the overflow I_{of}/I_{in} on the characteristic size of the soil particle d_m at various pressure values in the conveying branch pipe. From Fig. 5 it is seen that at values of $d_m > 20$ μm, as a result of the hydrocycloning, the pollutant concentration in the overflow sharply increases. In the underflow, on the contrary, the pollution intensity sharply decreases. Thus, as a result of the hydrocycloning, only separation products leaving the hydrocyclone through the overflow launder need to be cleaned, whereas those carried off by the underflow launder need no additional cleaning if adequate operating parameters of the hydrocyclone are chosen. This indicates that the application of hydrocyclones is highly promising for cleaning soils.

This work was supported by the RF Ministry of science, industry, and technologies (RF President's grant No. MD-197.2003.08) as well as by the Alexander von Humboldt foundation (Germany).

NOTATION

a, acceleration, m/sec^2; C_1, C_2, C_3, C_μ, parameters in the turbulence model; C_d, drag coefficient; C_Q, model constant; d_c, cyclone diameter, mm; d_{of} and d_{uf}, diameters of the overflow and underflow launders, mm; d_{in}, inlet diameter, mm; D_p, turbulent diffusion coefficient of particles, m/sec^2; D_t, turbulent diffusion coefficient of the carrier phase, m/sec^2; d_m, median diameter, m; d_p, particle diameter, m; E, model parameter; $F(\lambda)$, function of the relative film thickness; G, dissipative function, W/m^3; g, free fall acceleration, m/sec^2; I, degree of soil pollution; k, turbulent kinetic energy, m^2/sec^2; L, turbulence scale, m; L_1, cylindrical section length, mm; L_2, conic section length, mm; L_3, postcyclone length, mm; l, oil film thickness, μm; l_1, total length of the discharge pipe, mm; l_2, length of the part of the discharge pipe inserted into the hydrocyclone, mm; M_j, mass concentration of particles of the jth fraction; m, distribution constant; N, number of fractions of particles; p, pressure, Pa; Q, mass flow, kg/sec; $q_{of}(d_d)$, fraction of droplets of a given size leaving the hydrocyclone through the overflow launder; R_c, hydrocyclone radius, m; r, radial coordinate, m; Re, Reynolds number; Ri, Richardson number; Tu, turbulence intensity; u, axial velocity, m/sec; **V**, velocity vector, m/sec; v, radial velocity, m/sec; w, tangential velocity, m/sec; x, axial coordinate, m; Y, distance from the

wall; z_1, z_2, z_3, z_4, parameters in the equation of turbulent diffusion of particles; α, parameter inverse to the relaxation time of particles; β, parameter characterizing the relaxation path; γ, model constant; δ, distribution constant; ε, turbulent energy dissipation, W/kg; η, model constant; κ, von Karman constant; λ, relative thickness of oil film; μ, dynamic viscosity, Pa·sec; ρ, density, kg/m^3; σ_k, σ_ε, parameters in the turbulence model; $\sigma_{r\varphi}$, anisotropy coefficient; τ_w, wall stress, Pa; χ, correction factor in the resistance law; $\Psi(d_p)$, distribution function. Subscripts: c, cyclone; d, drag; ef, effective; in, inlet; liq, liquid; m, median; *n*w, nearest wall-adjacent node; of, overflow launder; oil, oil; p, particle; rel, relative; $r\varphi$, corresponding stress tensor component in the cylindrical coordinate system; sl, suspension; t, turbulent; uf, underflow launder.

REFERENCES

1. T. C. Monredon, K. T. Hsien, and R. K. Rajamani, Fluid flow model of the hydrocyclone: an investigation of device dimensions, *Int. J. Mineral Process*, **35**, No. 1, 65–83 (1992).
2. O. Matvienko, J. Dücк, and Th. Neeβe, Hydrodynamics and particle separation in the hydrocyclone, in: *Proc. 2nd Int. Symp. on Two-Phase Flow. Predictions and Experimentation*, May 23–26, 1999, Pisa, Italy (1999), pp. 923–928.
3. I. G. Dueck, O. V. Matvienko, and T. Neesse, Simulation of the hydrodynamics and separation in a hydrocyclone, *Teor. Osn. Khim. Tekhnol.*, **34**, No. 5, 478–488 (2000).
4. O. V. Matvienko, Analysis of the turbulence models and investigation of the structure of the flow in a hydrocyclone, *Inzh.-Fiz. Zh.*, **77**, No. 2, 58–64 (2004).
5. A. K. Gupta, D. G. Lilley, and N. Syred, *Swirling Flows* [Russian translation], Mir, Moscow (1987).
6. F. Boysan, Numerical modelling of cyclone separation, *Selected Topics in Two-Phase Flow. Lectures Series*, **9**, No. 1, Trondheim, Norway (1984), pp. 137–158.
7. Th. Neeβe and H. Schubert, Modellierung und verfahrenstechnische Dimensionierung der turbulenten Querstromklassierung. Teil I, *Chem. Techn.*, **27**, No 9, 529–533 (1975).
8. A. M. Kutepov (Ed.), *Processes and Apparatuses of Chemical Technology* [in Russian], Logos, Moscow (2002).
9. C. Crowe, M. Sommerfeld, and Ya. Tsuji, *Multiphase Flows with Droplets and Particles*, CRC Press (1998).
10. O. V. Matvienko and E. V. Evtyushkin, Mathematical modeling of the turbulent transfer of the dispersed phase in a turbulent flow, *Vestn. TGPU*, Issue 6 (43), 50–53 (2004).
11. A. I. Povarov, *Hydrocyclones at Concentrating Mills* [in Russian], Nedra, Moscow (1978).
12. L. Svarovsky, *Hydrocyclones*, Technomic Publishing, London (1984).
13. I. G. Ternovskii and A. M. Kutepov, *Hydrocycloning* [in Russian], Nauka, Moscow (1994).
14. H. Trawinski, Der Hydrozyclon als Hilfsgerat zur Grundstoffveredelung, *Chemie Ing. Techn.*, **25**, No. 6, 331–340 (1953).
15. S. Patankar, *Numerical Methods for Solving Problems of Heat Transfer and Dynamics of Fluid* [Russian translation], Énergoatomizdat, Moscow (1984).